Published in final edited form as:
Curr Opin Struct Biol. 2011 June ; 21(3): 327–334. doi:10.1016/j.sbi.2011.03.016.

Base ionization and ligand binding: how small ribozymes and riboswitches gain a foothold in a protein world*

Joseph A. Liberman and **Joseph E. Wedekind**†
Department of Biochemistry and Biophysics, and Center for RNA Biology, University of Rochester School of Medicine and Dentistry, Rochester, New York 14642

Abstract

Genome sequencing has produced thousands of non-protein coding (nc)RNA sequences including new ribozymes and riboswitches. Such RNAs are notable for their extraordinary functionality, which entails exquisite folding that culminates in biocatalytic or ligand-binding capabilities. Here we discuss advances in relating ncRNA form to function with an emphasis on base-pK_a shifting by the hairpin and hepatitis delta virus ribozymes. We then describe ligand binding by the two smallest riboswitches, which target preQ$_1$ and S-adenosyl-(L)-homocysteine, followed by an analysis of a second-messenger riboswitch that binds cyclic-di-GMP. Each riboswitch is then compared to a protein that binds the same ligand to contrast binding properties. The results showcase the breadth of functionality attainable from ncRNAs, as well as molecular features notable for antibacterial design.

Introduction

Non-coding RNAs (ncRNAs) are a ubiquitous class of molecules present in all three domains of life. Their activities include – but are not limited to – RNA processing (i.e. cleavage and ligation) as well as regulation of transcription, translation and splicing. Small ribozymes and riboswitches represent distinct classes of structured ncRNAs that have proven prevalent in genome-wide searches [1,2]. The defined biological activities of these molecules make them ideal to investigate relationships between RNA structure and function, which has implications for defining the catalytic principles of RNA [1] as well as the basis for gene regulation and targeting by antimicrobials [3–5].

The reaction of small ribozymes is one of nucleolytic transesterification (Figure 1A). Family members include the Varkud satellite (VS), hammerhead, hepatitis δ virus (HDV), glmS, and hairpin ribozymes, whose distinguishing characteristics include a diminutive size (≈ 80 nucleotides), and the ability to utilize reaction channels independent of multivalent ions [6,7]. As such, this family is ideal to investigate the roles of RNA bases in catalysis. At the outset, it would appear that ribozymes are poor candidates for acid-base chemistry since free nucleosides do not ionize at biological pH. However, it has been known for some time that ribozymes can alter base pK_a values [8,9], but the *extent of ionization* and *structural*

†Address correspondence to: Prof. Joseph E. Wedekind, 601 Elmwood Avenue, Box 712, Rochester New York 14642. Phone: (585) 273-4516; Fax: (585) 275-6007; joseph.wedekind@rochester.edu.

attributes contributing to this modulation represent significant knowledge gaps. Here, we review these topics with an emphasis on developments in microscopic pK_a measurements.

In some bacterial species RNA controls 4% of genes with riboswitches accounting for more than half of this regulation [10,11]. Riboswitches are organized functionally into a high-affinity aptamer domain that binds small molecule effectors, and a flanking expression platform that harbors gene regulatory sequences (Figure 1B) [12]. With 15 distinct small-molecule targets identified, the general riboswitch mechanism is to control access to transcriptional or translational sequences in the 5´-UTR of an associated mRNA through changes in secondary and tertiary structure upon ligand binding. Recently, two of the smallest riboswitch aptamer structures were determined – i.e. that of the hypermodified guanine preQ$_1$ and that of S-adenosyl-(L)-homocysteine (SAH) [13–16]. In addition, the first structure of a riboswitch that binds a second messenger, bis-(3´–5´)-cyclic dimeric GMP (c-di-GMP), was determined [17–19]. For the SAH and preQ$_1$ riboswitches, the preferred metabolite is selected over similar ligands by discrimination of a single functional group. Specifically the methyl donor group of SAM is sterically occluded in favor of SAH, whereas the methylamine group of preQ$_1$ engages in a hydrogen bond that is inaccessible to the preQ$_0$ nitrile moiety. Binding analysis of the c-di-GMP riboswitch indicated the ligand is essentially irreversibly bound on a biological timescale (dissociation t½ 44 d), although RNA polymerase is an important kinetic control factor that must also be considered. Finally, a comparison of each RNA aptamer to a protein that binds the same ligand revealed many commonalties. In the case of preQ$_1$, this analysis clarifies how preQ$_1$ binds preferentially over its metabolic precursor preQ$_0$ – remarkably, such a selectivity filter is observed in both RNA and protein.

Relating hairpin ribozyme microscopic pK_a measurements to function

The apparent pK_a of an enzymatic reaction can provide insight into the identity of chemical groups transferring protons in catalysis. Ambiguity arises if known functional groups do not titrate at values consistent with the apparent pK_a of the reaction [20]. Such is the case with small ribozymes, thereby necessitating the development of techniques to measure the pK_a of specific nucleobases to elucidate their potential to contribute to catalysis. Although NMR has been the cornerstone of the field, recent developments offer alternatives for measurements in solution, and in single crystals. Several small ribozymes of known structure including the glmS, hammerhead and hairpin possess guanine bases in their active sites that are invoked in catalysis (reviewed in [1]). To provide broader insight into guanine function, 8-azaguanine (8azaGua) was chosen as a fluorescent probe because its quantum yield changes in response to N1 protonation [21]. The hairpin ribozyme was selected as a model system since functional data and crystal structures place Gua8 and Ade38 in apposition to the scissile bond [22–24]. Using 8azaGua8, a pK_a of 9.95 ± 0.04 was measured in 1 mM $MgCl_2$, which is 1.4 log units higher than the 8azaGTP control. Notably, 9.95 is 3.45 log units higher than the apparent pK_a of the reaction [25], demonstrating that the imine at position 8 is not depressed as expected for optimal general base catalysis. This finding implies that Gua8 donates an imino hydrogen bond to stabilize the transition state [21], which concurs with abasic rescue experiments that argue for an electrostatic role of the base amidine moiety in cleavage as well as ligation (reviewed in [22]). An alternative explanation is that the very small fraction of Gua8 N1 ionized at biological pH can function in cleavage as a general base in concert with Ade38 [22,26]. At present, additional experiments are required to differentiate these possibilities, and we will touch on these later. We now shift our attention to Ade38, which is an essential base for efficient hairpin ribozyme activity [22].

Although Ade38 of the hairpin ribozyme is predicted to be protonated in both electrostatic stabilization and general acid catalysis proposals, no direct determination of the Ade38 pK_a was reported until recently. To this end Raman crystallography was employed, which can directly measure group-specific ionization properties in RNA crystals [27]. Due to the rich crystallographic history of the hairpin ribozyme [22], pK_a measurements were made using crystals of known, high-resolution structure. This strategy provides a means to empirically relate local structural changes with individual base pK_a perturbations (e.g. how does imino-group ionization change along a reaction coordinate captured as discrete precatalytic, transition-state, and product analogs). As a starting point, this technique was applied to crystals of the hairpin ribozyme in a precatalytic conformation [28]. As a negative control, N1-deaza-adenosine (N1dAde) was used because it is isosteric with adenosine but incapable of imino proton exchange. When substituted at position 38, the N1dAde hairpin ribozyme remained folded but was completely inactive [29]; in contrast, substitutions at positions 9 and 10 were relatively innocuous [30]. By evaluating changes in Raman spectra from crystals harboring the N1dAde38-variant or Ade38 over a range of pH values, it became clear that N1dAde38 crystals had no adenine imino groups shifted to neutrality, whereas wildtype crystals exhibited a single base with a pK_a of 5.46 ± 0.05. This value is higher than the pK_a of 3.68 ± 0.4 for AMP in solution [31], an effect ascribed to the close proximity of Ade38 imine to the scissile-bond oxygens [29,31]. However, the Ade38 N1 pK_a was still below the apparent pK_a of 6.5 for the reaction [22] suggesting that the precatalytic conformation is not completely 'fine-tuned' for chemistry or that Ade38 is not solely responsible for rate-limiting proton transfer. Structural changes in the hairpin ribozyme active site resulting from transition-state analogs may be better suited to elicit pK_a shifting toward the apparent pK_a of the reaction since more hydrogen bonds are donated from Ade38 to the scissile bond in the transition-state conformation [24,29].

The observation that the N1 moiety of Ade38 is shifted toward neutrality is important on several levels. First, protonation of Ade38 fulfills an important role in stabilizing the nearby O5´-leaving group, which is especially important for phosphodiester bond scission [20]. It is also safe to conclude that elevating the N1 pK_a of Ade38 by 1.8 log units is an effective precatalytic strategy to promote formation of the transition state (Figure 1A); in addition, the possibility that an ionized Ade38 depresses the pK_a of the nearby Gua8 O2´-nucleophile should not be overlooked [31]. However, despite advances in pK_a measurements, it is premature to definitively assign the functions of Gua8 and Ade38 in the hairpin ribozyme reaction.

Base ionization and metal binding in the HDV ribozyme

Crystallographic analyses of the HDV ribozyme have posited both general base and general acid roles for Cyt75 (reviewed in [32]), thus obfuscating the kinetic ambiguity inherent in the pH-rate data. To elucidate the role of Cyt75, Raman crystallography was applied to the HDV ribozyme in a series of pioneering experiments that measured the pK_a of Cyt75 as 6.40 ± 0.05 in single crystals containing 2 mM Mg^{2+}. This value is shifted significantly toward neutrality relative to CMP whose N3 pK_a is 4.09 ± 0.4 [33]. Moreover, Cyt75-base ionization in crystals coupled anti-cooperatively with Mg^{2+} concentration in a manner that mirrors pH-rate experiments in solution [33]. Such coupling implies close spatial proximity, which came into focus with the determination of a new crystal structure. This 1.9 Å resolution HDV ribozyme revealed a novel G-U reverse wobble pair coordinating $Mg(H_2O)n^{2+}$ in the active site [34]. Although the Uri-*1* nucleoside of the scissile bond was disordered, a precleavage model was created that is consistent with biochemical observations (Figure 1C). N3 of Cyt75 is poised to donate a proton to the O5´-leaving group, whereas $Mg(H_2O)n^{2+}$ is compatible with inner-sphere coordination to the O2´-nucleophile and *pro-*R_p oxygen of the scissile bond. This model places Cyt75 N3 and Mg^{2+} within 5.5

Å, which supports a mechanism wherein Mg^{2+} is a Lewis acid and Cyt75 is a general acid in cleavage. This hybrid catalytic strategy combines features of both large and small ribozymes making it especially applicable to understanding a wide spectrum of RNA catalysts.

The $preQ_1$ riboswitch is an economical aptamer that uses hydrogen bonds for ligand specificity

Queuosine (Q) is a hypermodifed guanosine that confers translational fidelity [35]. Only bacteria synthesize Q de novo whereas eukaryotes obtain its base form, queuine, as a nutrient that is exchanged for guanine in tRNA [36]. Synthesis of Q is regulated in Firmicutes by the smallest known riboswitch aptamer, a 34-mer that binds the Q precursor $preQ_1$. The aptamer is located in the 5′-UTR of genes encoding proteins necessary for Q biosynthesis or $preQ_1$ import [37]. Structures of the $preQ_1$ riboswitch have been solved in the presence of $preQ_1$ for the *Bacillus subtilis* aptamer [13,14] and bound to the $preQ_1$ antecedent $preQ_0$ for the *Thermoanaerobacter tengcongensis* aptamer [15]. The aptamer structures are highly compact, H-type pseudoknots that harbor the metabolite-binding site in a core stem-loop. A ‘belt’ of hydrogen bonds recognizes the ligand wherein conserved base Cyt15 is the main specificity determinant [37] (Figure 2A); bases Uri6 and Ade29 recognize the minor-groove edge (Figure 2A) and these interactions are preserved for $preQ_0$ (Figure 2A, *inset*). The affinities of $preQ_1$ and $preQ_0$ have been determined by equilibrium dialysis to be ≈ 20 nM and 100 nM, respectively, for a 52-mer construct [37] but may differ by as much as 20-fold (Jenkins & Wedekind, *unpublished*). At present, the molecular basis for selectivity is uncertain. One possibility is that the bent methylamine of $preQ_1$ interacts with O6 and N7 of Gua5 (not shown) [13,14]. By contrast, the nitrile group of $preQ_0$ is linear and unbendable, precluding such hydrogen bonds [15]. In the *B. subtilis* structures, the methylamine hydrogen bonds to the phosphate backbone [13,14], although this interaction is absent in the *T. tengcongensis* structure (PDB entry 3Q50). Base stacking above and below the hydrogen-bond belt arises from Gua11 on the loop side (Figure 2A) and a conserved Cyt16-Gua5 base pair on the stem side (not shown).

Recognition of $preQ_1$ by the RNA aptamer parallels the mode of substrate binding by tRNA-guanine transglycosylase (TGTase), an enzyme that exchanges Gua34 with $preQ_1$ in tRNA to yield Q [36]. Gln203 and Asp156 of TGTase recognize the Watson-Crick face of the metabolite comparable to Cyt15 (Figures 2A and 2B). Asp102 confers further specificity at the minor-groove edge of $preQ_1$, analogous to Ade29; no TGTase interaction is comparable to Uri6. $PreQ_1$ specificity is bolstered by interactions with the backbone amide of Gly230 and the side-chain of Gln203, which interact with the ligand O6 keto. In vitro assays demonstrated that $preQ_1$ and $preQ_0$ each serve as substrates for TGTase [38]. Whereas the methylamine of $preQ_1$ hydrogen bonds to the carbonyl oxygen of Leu231, the $preQ_0$ nitrile forms a bifurcated hydrogen bond with the backbone amides of Ala232 and Leu231. Like Gua11, Tyr106 abuts the metabolite for aromatic stacking (Figure 2B versus 2A); Met260 serves as a hydrophobic buttress equivalent to the Cyt16-Gua5 base pair. Unlike the riboswitch, TGTase binds both $preQ_1$ and $preQ_0$ with a similar affinity (K_M 700 nM and 900 nM for $preQ_1$ and $preQ_0$, respectively), but the apparent rate constant is 10-fold lower for $preQ_0$ [38]. Our calculations show that TGTase buries slightly more $preQ_1$ surface area (330 $Å^2$ of 337 $Å^2$) than the riboswitch (297 $Å^2$ buried). Substrate sequestration by TGTase likely shields the reaction from solvent, whereas the riboswitch requires high affinity and specificity to control accessibility to gene regulatory signals on a biological timescale. Careful measurements of kinetic constants associated with ligand binding and release represent priority experiments for riboswitches since equilibrium K_D values are unlikely to reflect the metabolite concentrations necessary to elicit half-maximal transcription termination *in vivo* [39].

The S-adenosyl-(L)-homocysteine riboswitch uses steric selectivity

A second, minimal RNA aptamer is the 46-mer SAH riboswitch. This motif upregulates SAH hydrolase or 5-methyltetrahydrofolate-homocysteine methyltransferase in response to cellular SAH levels [40]. The aptamer is the first of its class and exhibits as much as 1,000-fold discrimination over S-adenosyl-(L)-methionine (SAM) [40]. Recently, a crystal structure of this riboswitch was determined revealing an LL-type pseudoknot [16]. Ligand binding occurs by intercalation of the SAH adenine ring between Ade29 and Cyt16 (Figure 2C). However, unlike $preQ_1$, no direct interaction is made to the Watson-Crick face of SAH. Instead, a sheared pair exists between the adenine moiety and Gua15 (Figure 2C). The amino group of homocysteine hydrogen bonds to N3 of Gua47 and a phosphate oxygen of Gua30, whereas its carboxylic acid hydrogen bonds to the respective 2′-OH groups of Gua31 and Gua47. Selectivity for SAH is achieved by excluding the thioether of SAM, which would clash with C4′ of Ade29 and N7 of Gua31 [16]. As such, the SAH riboswitch uses steric selectivity rather than electrostatics as a specificity gate [16].

BchU is a methyl transferase whose reaction expends SAM yielding SAH. The BchU-SAH complex has been described [41] and exhibits twice as many interactions to the ligand as the SAH riboswitch. The adenine moiety of SAH packs against Leu201 and Ile228 analogous to base stacking in the riboswitch (Figures 2C and 2D). Specificity for the adenine of SAH is achieved by N6 and N1 base interactions to Asp156 and Ile228, respectively. The absence of an enzyme interaction with N7 of SAH differentiates it from the riboswitch. Similarly, BchU hydrogen bonds to the 2′- and 3′-OH groups of SAH via Asn200 and Glu147, respectively, which has no equivalent in the aptamer. Turning now to the homocysteine moiety of SAH, the riboswitch and enzyme show many shared interaction points. The amino group of homocysteine hydrogen bonds to the carbonyl oxygens of Gly177 and Cys242, whereas the carboxyl group hydrogen bonds to the Cys242 thiol and the guanidinium group of Arg243 (Figure 2D). In contrast, a non-bonded contact between the His150 imidazole and the SAH sulfur represents a unique interaction not observed in the riboswitch. Although BchU affinity for SAH has not been reported, it sequesters more ligand surface (551 $Å^2$ of 595 $Å^2$) than the riboswitch (430 $Å^2$ buried), which binds SAH with an apparent K_D of 32 nM [16]. These observations provide benchmarks for the requirements for active site sequestration and gene regulation, respectively, and demonstrate the elegance by which an RNA aptamer discriminates against a single methyl group.

The cyclic-di-GMP riboswitch as a model for second-messenger regulation

The c-di-GMP riboswitch binds a second messenger rather than a metabolite and regulates cellular processes such as the transition from a motile to a stationary state [42]. Independent crystal structures of the *Vibrio cholerae* aptamer revealed a three-helix, Y-shaped fold with a binding pocket located at the helical junction [17,18]. A 2.3 Å resolution structure containing Mg^{2+} indicated the metal hydration sphere contacts the non-bridging c-di-GMP phosphate oxygens at nucleotide G_α (Figure 2E), whereas those of G_β are solvent exposed [19]. Ade47 of the riboswitch intercalates between the bases of c-di-GMP providing aromatic stacking. The outside face of each c-di-GMP base packs against the aptamer with Gua14 positioned near G_β and the Gua21-Cyt46 pair abuts G_α (not shown). Extensive hydrogen bonds from the aptamer dictate specificity with the $G_\beta$base pairing to Cyt92 and its N3 imino interacting with the N4 of Cyt17; G_α Hoogsteen pairs with Gua20, and its exocylic amine hydrogen bonds to a non-bridging oxygen of Ade49 and the 2′-OH of Cyt46.

Proteins with a PilZ domain recognize c-di-GMP, which induces ligand-dependent conformational changes [43]. Structural studies of PilZ bound to c-di-GMP [44] show striking similarities to its riboswitch counterpart with a notable exception. Namely, the

riboswitch binds c-di-GMP with the guanine bases in a stereochemically “eclipsed” conformation, whereas PilZ binds with the bases “staggered” such that they do not overlap each other (Figure 2E and 2F). Beyond this difference, recognition of the Watson-Crick face of G_β is similarly replete with hydrogen bonds including Ser164, Asp162 and Arg169; additional interactions occur with N7 and a non-bridging oxygen, which coordinate the amide side-chain of Asn208. Finally, the ε-amino of Lys137 hydrogen bonds with the 3′-oxygen of G_β. G_α is recognized by hydrogen bonds from Arg136 to its Hoogsteen face like Gua20 of the riboswitch. A second arginine at position 140 interacts with the non-bridging oxygens of G_α; its guanidinium group resides above G_β in a cation-π stack spatially analogous to Ade47 in the riboswitch. Not surprisingly, both the PilZ domain and the RNA aptamer sequester comparable ligand surface areas with 577 $Å^2$ versus 664 $Å^2$ buried of ≈ 800 $Å^2$ total, respectively. The apparent K_D values for c-di-GMP differ significantly with the PilZ domain binding at 100–300 nM [44] and the riboswitch binding at 11 pM [17]. To be effective in gene regulation, the riboswitch is likely to be kinetically controlled such that its slow on-rate allows it to respond linearly to c-di-GMP over a wide range of concentrations significantly above the K_D and on a timescale conducive to transcriptional control [17]. Other factors worth future exploration include the interaction between the riboswitch and the polymerase itself [39].

Conclusions and future prospects

The ribozymes and riboswitches presented here are illustrative of the diversity and functional elegance typical of structured ncRNAs. Although small ribozyme mechanisms appear well developed, structural information cannot always be reconciled with function. As such, new fluorescent and Raman crystallographic approaches serve to pinpoint and quantify shifts in base pK_a values, providing a greater understanding of how conformational changes fine-tune ionization for catalysis. These data provide benchmarks for calculations that require pK_a values to simulate chemical mechanisms [45]. Additional efforts should look to the use of sulfur probes to assess the importance of leaving-group lability [46], which can shed light on the assignment of general acid catalysts [46,47]. Recent advances in the application of kinetic isotope effects [48] demonstrate the feasibility of examining ribozyme transition-state structures. The utility of this approach has been proven for protein enzymes [49].

Although small ribozymes made an impressive showing in a multigenome analysis [50], there is no end in sight for the number of riboswitches, whose structural diversity far exceeds its known small-molecule-target repertoire [2]. These regulatory elements are likely so prominent because of their economical organization, as well as their ability to discriminate ligands at the level of single functional groups, as observed for the $preQ_1$ and SAH aptamers. Significantly, a comparison of $preQ_1$ riboswitches indicated common molecular features for ligand targeting between genera. Moreover, although ribozymes and proteins utilize the same types of binding interactions, key differences exist such as the use of positively charged side chains by proteins and metallo-based recognition by riboswitches seen for c-di-GMP. These characteristics are notable for structure-guided inhibitor design, which represents an emergent frontier for antibacterial discovery [51].

Acknowledgments

We thank Jason Salter, Jermaine Jenkins, Jolanta Krucinska, Robert Spitale and Geoffrey Lippa for helpful comments and ideas. We express gratitude to Barbara Golden for model coordinates of the HDV ribozyme, and the National Institutes of Health for grants R01-GM063162 and S10-RR026501 to JEW.

References and recommended reading

Papers of particular interest, published within the annual period of review, have been highlighted as:

• of special interest

•• of outstanding interest

1. Wedekind, JE. Metal Ion Binding and Function in Natural and Artificial Small RNA Enzymes from a Structural Perspective. In: Sigel, A.; Sigel, H.; Sigel, R., editors. Met. Ions Life Sci.: Structural and Catalytic Roles of Metal Ions in RNA. Royal Society of Chemistry; 2011. p. 299-345.
2. Weinberg Z, Wang JX, Bogue J, Yang J, Corbino K, Moy RH, Breaker RR. Comparative genomics reveals 104 candidate structured RNAs from bacteria, archaea, and their metagenomes. Genome Biol. 2010; 11:R31. [PubMed: 20230605]
3. Lee ER, Blount KF, Breaker RR. Roseoflavin is a natural antibacterial compound that binds to FMN riboswitches and regulates gene expression. RNA Biol. 2009; 6:187–194. [PubMed: 19246992]
4. Serganov A, Patel DJ. Amino acid recognition and gene regulation by riboswitches. Biochim Biophys Acta. 2009; 1789:592–611. [PubMed: 19619684]
5. Blount KF, Wang JX, Lim J, Sudarsan N, Breaker RR. Antibacterial lysine analogs that target lysine riboswitches. Nat Chem Biol. 2007; 3:44–49. [PubMed: 17143270]
6. Murray JB, Seyhan AA, Walter NG, Burke JM, Scott WG. The hammerhead, hairpin and VS ribozymes are catalytically proficient in monovalent cations alone. Chem. Biol. 1998; 5:587–595. [PubMed: 9818150]
7. Nakano S, Proctor DJ, Bevilacqua PC. Mechanistic characterization of the HDV genomic ribozyme: assessing the catalytic and structural contributions of divalent metal ions within a multichannel reaction mechanism. Biochemistry. 2001; 40:12022–12038. [PubMed: 11580278]
8. Nakano S, Chadalavada DM, Bevilacqua PC. General acid-base catalysis in the mechanism of a hepatitis delta virus ribozyme. Science. 2000; 287:1493–1497. [PubMed: 10688799]
9. Perrotta AT, Shih I, Been MD. Imidazole rescue of a cytosine mutation in a self-cleaving ribozyme. Science. 1999; 286:123–126. [PubMed: 10506560]
10. Winkler WC, Breaker RR. Regulation of bacterial gene expression by riboswitches. Annu Rev Microbiol. 2005; 59:487–517. [PubMed: 16153177]
11. Irnov, Kertsburg A, Winkler WC. Genetic control by cis-acting regulatory RNAs in Bacillus subtilis: general principles and prospects for discovery. Cold Spring Harb Symp Quant Biol. 2006; 71:239–249. [PubMed: 17381303]
12. Montange RK, Batey RT. Riboswitches: emerging themes in RNA structure and function. Annu Rev Biophys. 2008; 37:117–133. [PubMed: 18573075]
13. Klein DJ, Edwards TE, Ferré-D'Amaré AR. Cocrystal structure of a class I preQ1 riboswitch reveals a pseudoknot recognizing an essential hypermodified nucleobase. Nat Struct Mol Biol. 2009; 16:343–344. [PubMed: 19234468] The crystal structure of the *B. subtilis* riboswitch bound to $preQ_1$ provides an example of transcriptional control by the smallest class I aptamer.
14. Kang M, Peterson R, Feigon J. Structural Insights into riboswitch control of the biosynthesis of queuosine, a modified nucleotide found in the anticodon of tRNA. Mol Cell. 2009; 33:784–790. [PubMed: 19285444] A careful analysis of ligand-dependent folding is provided.
15. Spitale RC, Torelli AT, Krucinska J, Bandarian V, Wedekind JE. The structural basis for recognition of the PreQ0 metabolite by an unusually small riboswitch aptamer domain. J Biol Chem. 2009; 284:11012–11016. [PubMed: 19261617] The crystal structure of the *T. tengcongensis* riboswitch aptamer in complex with the $preQ_1$ precursor, $preQ_0$. This class I aptamer provides an example of translational control.
16. Edwards AL, Reyes FE, Heroux A, Batey RT. Structural basis for recognition of S-adenosylhomocysteine by riboswitches. RNA. 2010; 16:2144–2155. [PubMed: 20864509] This is the only known structure of an SAH riboswitch. The mode of ligand binding utilizes steric rather than electrostatic means to select SAH over SAM, which is supported by the accompanying biochemical analysis.

17. Smith KD, Lipchock SV, Ames TD, Wang J, Breaker RR, Strobel SA. Structural basis of ligand binding by a c-di-GMP riboswitch. Nat Struct Mol Biol. 2009; 16:1218–1223. [PubMed: 19898477]

18. Kulshina N, Baird NJ, Ferre-D'Amare AR. Recognition of the bacterial second messenger cyclic diguanylate by its cognate riboswitch. Nat Struct Mol Biol. 2009; 16:1212–1217. [PubMed: 19898478]

19. Smith KD, Lipchock SV, Livingston AL, Shanahan CA, Strobel SA. Structural and Biochemical Determinants of Ligand Binding by the c-di-GMP Riboswitch. Biochemistry. 2010; 49:7351–7359. [PubMed: 20690679] A high-resolution crystal structure of the c-di-GMP riboswitch in the presence of Mg^{2+} showing involvement of the metal in ligand binding. A supporting analysis is presented on the effects of riboswitch mutants on ligand-binding.

20. Bevilacqua PC. Mechanistic considerations for general acid-base catalysis by RNA: revisiting the mechanism of the hairpin ribozyme. Biochemistry. 2003; 42:2259–2265. [PubMed: 12600192]

21. Liu L, Cottrell JW, Scott LG, Fedor MJ. Direct measurement of the ionization state of an essential guanine in the hairpin ribozyme. Nat Chem Biol. 2009; 5:351–357. [PubMed: 19330013] The development and application of 8-azaguanine in the direct measurement of the Gua8 pK_a is described. This work has implications for hairpin ribozyme general base catalysis, and broader implications for probing ribozyme mechanisms of action.

22. Fedor MJ. Comparative enzymology and structural biology of RNA self-cleavage. Annu Rev Biophys. 2009; 38:271–299. [PubMed: 19416070]

23. Rupert PB, Massey AP, Sigurdsson ST, Ferre-D'Amare AR. Transition state stabilization by a catalytic RNA. Science. 2002; 298:1421–1424. [PubMed: 12376595]

24. Torelli AT, Krucinska J, Wedekind JE. A comparison of vanadate to a 2'-5' linkage at the active site of a small ribozyme suggests a role for water in transition-state stabilization. RNA. 2007; 13:1052–1070. [PubMed: 17488874]

25. Kuzmin YI, Da Costa CP, Cottrell JW, Fedor MJ. Role of an active site adenine in hairpin ribozyme catalysis. J Mol Biol. 2005; 349:989–1010. [PubMed: 15907933]

26. Wilson TJ, Lilley DM. Do the hairpin and VS ribozymes share a common catalytic mechanism based on general acid-base catalysis? A critical assessment of available experimental data. RNA. 2010; 17:213–221. [PubMed: 21173201]

27. Gong B, Chen JH, Yajima R, Chen Y, Chase E, Chadalavada DM, Golden BL, Carey PR, Bevilacqua PC. Raman crystallography of RNA. Methods. 2009; 49:101–111. [PubMed: 19409996]

28. Salter J, Krucinska J, Alam S, Grum-Tokars V, Wedekind JE. Water in the active site of an all-RNA hairpin ribozyme and effects of Gua8 base variants on the geometry of phosphoryl transfer. Biochemistry. 2006; 45:686–700. [PubMed: 16411744]

29. Spitale RC, Volpini R, Heller MG, Krucinska J, Cristalli G, Wedekind JE. Identification of an imino group indispensable for cleavage by a small ribozyme. J Am Chem Soc. 2009; 131:6093–6095. [PubMed: 19354216]

30. Spitale RC, Volpini R, Mungillo MV, Krucinska J, Cristalli G, Wedekind JE. Single-atom imino substitutions at A9 and A10 reveal distinct effects on the fold and function of the hairpin ribozyme catalytic core. Biochemistry. 2009; 48:7777–7779. [PubMed: 19634899]

31. Guo M, Spitale RC, Volpini R, Krucinska J, Cristalli G, Carey PR, Wedekind JE. Direct Raman measurement of an elevated base pKa in the active site of a small ribozyme in a precatalytic conformation. J Am Chem Soc. 2009; 131:12908–12909. [PubMed: 19702306] A Raman crystallography measurement of the Ade38 imino pK_a of the hairpin ribozyme. Knowledge of the high-resolution precatalytic structure allowed direct correlations to be made between structure and function with implications for general acid catalysis.

32. Das SR, Fong R, Piccirilli JA. Nucleotide analogues to investigate RNA structure and function. Curr Opin Chem Biol. 2005; 9:585–593. [PubMed: 16242990]

33. Gong B, Chen JH, Chase E, Chadalavada DM, Yajima R, Golden BL, Bevilacqua PC, Carey PR. Direct measurement of a pK(a) near neutrality for the catalytic cytosine in the genomic HDV ribozyme using Raman crystallography. J Am Chem Soc. 2007; 129:13335–13342. [PubMed: 17924627] The first description of the microscopic pK_a determination of a ribozyme base by

Raman crystallography with a careful analysis of the anti-cooperative coupling between tha imino pK_a of Cyt75 and Mg^{2+} levels.

34. Chen JH, Yajima R, Chadalavada DM, Chase E, Bevilacqua PC, Golden BL. A 1.9 Å crystal structure of the HDV ribozyme precleavage suggests both Lewis acid and general acid mechanisms contribute to phosphodiester cleavage. Biochemistry. 2010; 49:6508–6518. [PubMed: 20677830] The structure of a new HDV ribozyme in which a hydrated Mg^{2+} is located near a novel G-U pair. A model is described for Lewis -acid assisted catalysis with Cyt75 serving as a general acid.
35. Iwata-Reuyl D. Biosynthesis of the 7-deazaguanosine hypermodified nucleosides of transfer RNA. Bioorg Chem. 2003; 31:24–43. [PubMed: 12697167]
36. Grosjean H, de Crecy-Lagard V, Bjork GR. Aminoacylation of the anticodon stem by a tRNA-synthetase paralog: relic of an ancient code? Trends Biochem Sci. 2004; 29:519–522. [PubMed: 15450604]
37. Roth A, Winkler WC, Regulski EE, Lee BW, Lim J, Jona I, Barrick JE, Ritwik A, Kim JN, Welz R, et al. A riboswitch selective for the queuosine precursor preQ1 contains an unusually small aptamer domain. Nat Struct Mol Biol. 2007; 14:308–317. [PubMed: 17384645]
38. Tidten N, Stengl B, Heine A, Garcia GA, Klebe G, Reuter K. Glutamate versus glutamine exchange swaps substrate selectivity in tRNA-guanine transglycosylase: insight into the regulation of substrate selectivity by kinetic and crystallographic studies. J Mol Biol. 2007; 374:764–776. [PubMed: 17949745]
39. Wickiser JK, Winkler WC, Breaker RR, Crothers DM. The speed of RNA transcription and metabolite binding kinetics operate an FMN riboswitch. Mol Cell. 2005; 18:49–60. [PubMed: 15808508]
40. Wang JX, Lee ER, Morales DR, Lim J, Breaker RR. Riboswitches that sense S-adenosylhomocysteine and activate genes involved in coenzyme recycling. Mol Cell. 2008; 29:691–702. [PubMed: 18374645]
41. Wada K, Yamaguchi H, Harada J, Niimi K, Osumi S, Saga Y, Oh-Oka H, Tamiaki H, Fukuyama K. Crystal structures of BchU, a methyltransferase involved in bacteriochlorophyll c biosynthesis, and its complex with S-adenosylhomocysteine: implications for reaction mechanism. J Mol Biol. 2006; 360:839–849. [PubMed: 16797589]
42. Sudarsan N, Lee ER, Weinberg Z, Moy RH, Kim JN, Link KH, Breaker RR. Riboswitches in eubacteria sense the second messenger cyclic di-GMP. Science. 2008; 321:411–413. [PubMed: 18635805]
43. Schirmer T, Jenal U. Structural and mechanistic determinants of c-di-GMP signalling. Nat Rev Microbiol. 2009; 7:724–735. [PubMed: 19756011]
44. Benach J, Swaminathan SS, Tamayo R, Handelman SK, Folta-Stogniew E, Ramos JE, Forouhar F, Neely H, Seetharaman J, Camilli A, et al. The structural basis of cyclic diguanylate signal transduction by PilZ domains. EMBO J. 2007; 26:5153–5166. [PubMed: 18034161]
45. Moser A, Range K, York DM. Accurate proton affinity and gas-phase basicity values for molecules important in biocatalysis. J Phys Chem B. 2010; 114:13911–13921. [PubMed: 20942500]
46. Li NS, Frederiksen JK, Koo SC, Lu J, Wilson TJ, Lilley DM, Piccirilli JA. A general and efficient approach for the construction of RNA oligonucleotides containing a 5'-phosphorothiolate linkage. Nucleic Acids Res. 2010
47. Wilson TJ, Li NS, Lu J, Frederiksen JK, Piccirilli JA, Lilley DM. Nucleobase-mediated general acid-base catalysis in the Varkud satellite ribozyme. Proc Natl Acad Sci U S A. 2010; 107:11751–11756. [PubMed: 20547881] Replacement of the O5´-leaving group with sulfur in the VS ribozyme active provides support that Ade756 serves as a general acid in the cleavage reaction. An earlier precedent for this approach was set using the HDV ribozyme.
48. Harris ME, Dai Q, Gu H, Kellerman DL, Piccirilli JA, Anderson VE. Kinetic isotope effects for RNA cleavage by 2'-O- transphosphorylation: nucleophilic activation by specific base. J Am Chem Soc. 2010; 132:11613–11621. [PubMed: 20669950] The first description of kinetic isotope effects applied to general base catalyzed RNA cleavage. This work has implications for probing the transition states of ribozymes.

49. Schwartz SD, Schramm VL. Enzymatic transition states and dynamic motion in barrier crossing. Nat Chem Biol. 2009; 5:551–558. [PubMed: 19620996]

50. Webb CH, Riccitelli NJ, Ruminski DJ, Luptak A. Widespread occurrence of self-cleaving ribozymes. Science. 2009; 326:953. [PubMed: 19965505]

51. Kim JN, Blount KF, Puskarz I, Lim J, Link KH, Breaker RR. Design and antimicrobial action of purine analogues that bind Guanine riboswitches. ACS Chem Biol. 2009; 4:915–927. [PubMed: 19739679]

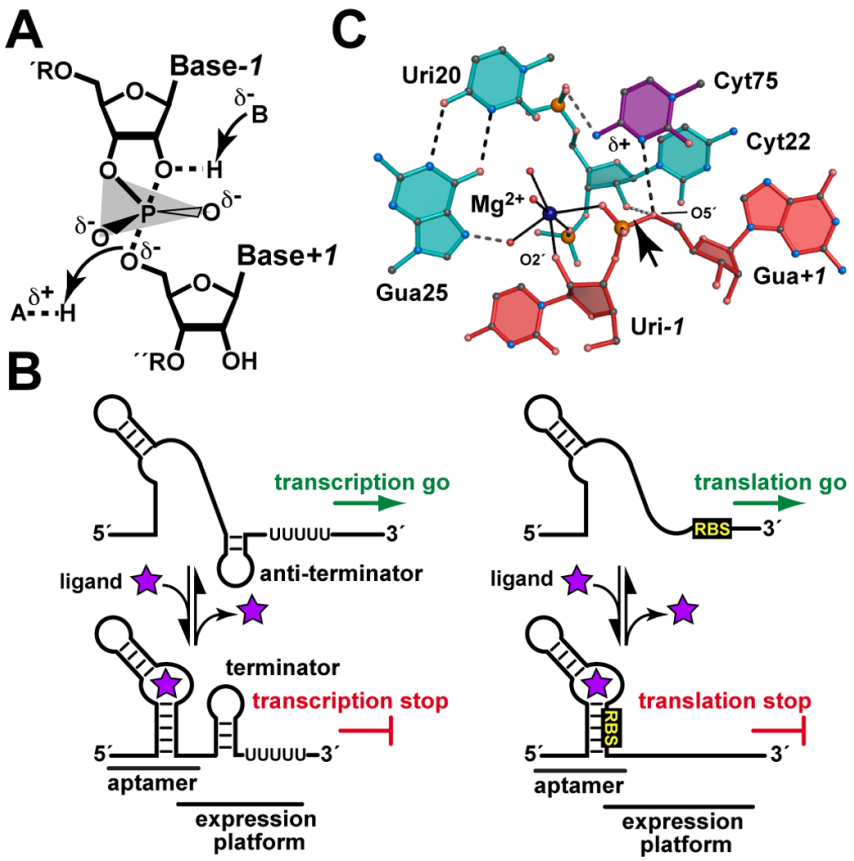

Figure 1. Biological activities and organization of small ribozymes and riboswitches

(**A**) The chemical reaction of small ribozymes is comparable to the first step of RNA cleavage by ribonuclease A. The transition state for the concerted reaction is depicted whereby general base B abstracts a proton from the O2´-nucleophile with charge transfer onto the O5´-leaving group that is ameliorated by general acid A. Positively charged groups that interact with the non-bridging oxygens of the oxyphosphorane are favorable. (**B**) Typical transcription and translational regulation by bacterial riboswitches. When cellular concentrations of ligand are low, signals in the 5´-UTR (untranslated region) or leader sequence of the mRNA are receptive to transcription (i.e. an anti-terminator stemloop is present) or translation (i.e. the ribosome binding site, denoted RBS, is exposed) of the downstream gene. When ligand levels rise, the aptamer binds its cognate small molecule shifting the equilibrium to an aptamer fold that sequesters RNA sequences in the expression platform necessary for transcription or translation. (**C**) Model of the precatalytic HDV ribozyme adapted from ref. [34]. The O2´-nucleophile and O5´-leaving group are labeled; an arrow indicates the scissile bond. Here the nucleophile coordinates directly to $Mg(H_2O)n^{2+}$, but outer sphere coordination is possible. The location of the protonated Cyt75 imine is depicted by “δ+”.

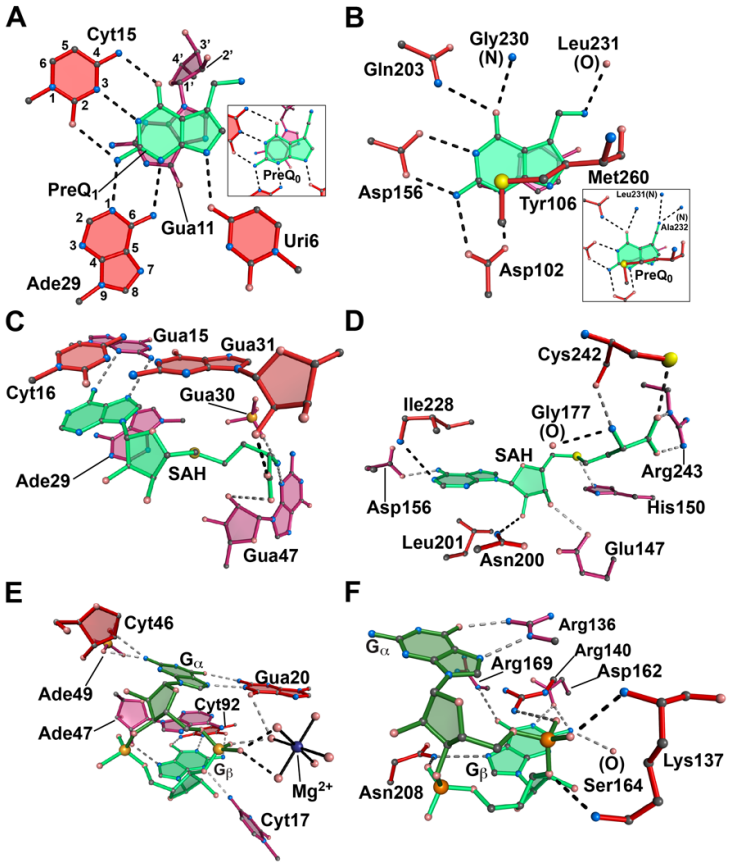

Figure 2. Comparison of riboswitches and proteins that bind a common ligand

(**A**) The metabolite-binding site of the class I preQ$_1$ riboswitch in complex with preQ$_1$ from *T. tengcongensis*. *Inset*: The same aptamer in complex with preQ$_0$. The respective PDB codes are 3Q50 and 3GCA. The atoms have been numbered for representative purine and pyrimidine bases according to IUPAC-IUB nomenclature. (**B**) The active site of the enzyme tRNA-guanine transglycosylase (TGTase) from *Z. mobilis* in complex with preQ$_1$. *Inset*: The same enzyme in complex with preQ$_0$. The respective PDB codes are 1P0E and 1P0B. (**C**) The metabolite-binding site of the SAH riboswitch from *R. solanacearum* in complex with SAH. The PDB code is 3NPQ. (**D**) The active site of the BchU methyltransferase from *C. tepidum* bound to SAH. The PDB code is 1X1B. (**E**) The c-di-GMP riboswitch aptamer from *Vibrio cholerae* in complex with the second messenger c-di-GMP. The PDB code is 3MXH. A hydrated Mg^{2+} is shown (blue) with solid lines drawn to waters (pink spheres) in the inner coordination sphere. (**F**) The PilZ domain (VCA0042) from *Vibrio cholerae* in complex with c-di-GMP. The PDB code is 2RDE. All ligands are depicted in shades of green. Nucleotides and amino acids of the binding pockets are shown in shades of burgundy to indicate depth; red is the topmost layer and crimson is at the bottom. Dashed lines signify putative hydrogen bonds.